Information Fusion using Particles Intersection

Ben-Gurion University
Department of Mechanical Engineering

Or Tslil | Avishy Carmi | Ben-Gurion University, Department of Mechanical Engineering

Abstract

A technique is presented for combining arbitrary empirical probability density estimates whose interdependencies are unspecified. The underlying estimates may be, for example, the particle approximations of a pair of particle filters. In this respect, our approach provides a way to obtain a new particle approximation, which is better in a precise information-theoretic sense than that of any of the particle filters alone. The viability of the proposed approach is demonstrated in a multiple object tracking scenario and robots localizations scenario.

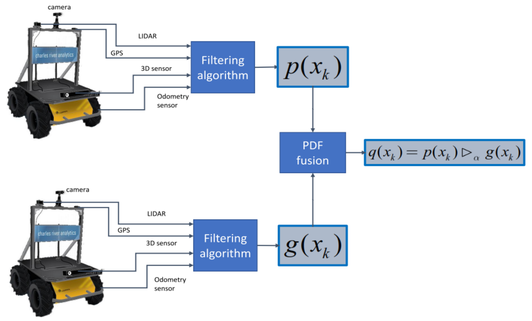

Figure 1: Example of the Information fusion in a multi-estimators scenario. Two robots try to localize with multiple sensors, each robot fuse the information from those sensor to produce an estimate of its location. The output of the filtering algorithm is a probability density function (pdf) and its expectation is the estimated state. $p(x)$ and $g(x)$ are the PDF's of the two robots estimators. We wish to obtain the fusion of both estimators while the correlations between the estimators are unknown.

Fusion of PDF Estimators

Let $p(x)$ and $g(x)$ be estimators of pdf $h(x)$, $q(x)$ is the fusion of $p(x)$ and $g(x)$:

$$q(x) = \frac{p(x) \triangleright_\alpha g(x)}{e^{-I_\alpha(p,g)}} \tag{1}$$

Where the operator $p(x) \triangleright_\alpha g(x) \triangleq p(x)^\alpha g(x)^{1-\alpha}$ is the log-convex combination of the two pdfs, and $I_\alpha(p,g) \triangleq -\log \int p(y)^\alpha g(y)^{1-\alpha} dy$ is the Chernoff information of $p(x)$ and $g(x)$. The three density estimators satisfy,

$$\mathrm{KL}\left(q \parallel h\right) = \underbrace{\alpha \mathrm{KL}\left(p \parallel h\right) + (1-\alpha)\mathrm{KL}\left(g \parallel h\right)}_{unknown} - I_\alpha(p,g) \tag{2}$$

where $\mathrm{KL}\left(q \parallel h\right) \overset{\text{def}}{=} \int q(x) \log(q(x)/h(x)) dx$ is the Kullback-Leibler (KL) divergence of $q(x)$.

Theorem 1 (Consistency of KL)**.** *There exists an* $\alpha \in [0,1]$ *for which*

$$\mathrm{KL}\left(q \parallel h\right) \leq \min\left\{\mathrm{KL}\left(p \parallel h\right), \mathrm{KL}\left(g \parallel h\right)\right\} \tag{3}$$

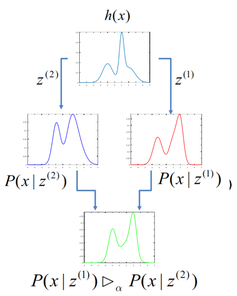

Figure 2: Illustration of the Gaussian mixture fusion steps. The blue and red lines are the Gaussian mixtures $f(x)$ and $g(x)$, and the green is their fusion by equation 1.

Particles Intersection

We name particles intersection the application of (1) using the empirical pdf representations obtained by a pair of PFs. The output of a conventional PF is a set of N samples (particles) which together provide an empirical estimate of the underlying filtering pdf,

$$\pi(x_k \mid z_{0:k}) = \sum_{i=1}^{N} w_k^{(i)} \delta(x_k - x_k^{(i)}) \tag{4}$$

It now follows that $q(x_k)$ vanishes unless x_k coincides with the same particle in both sets, $\{x_k^{(i),1}\}_i$ and $\{x_k^{(i),2}\}_i$, where $\{x_k^{(i),j}\}_i$ is the particles approximation of the jth PF. This issue may be alleviated by using instead

$$\pi_r(x_k \mid z_{0:k}^j) = \sum_{i=1}^{N} w_k^{(i),j} \exp\left\{-\beta \parallel x_k - x_k^{(i),j} \parallel_2^2\right\} \tag{5}$$

for $j = 1, 2$, where $\beta > 0$ is a regularization parameter, and $\| \cdot \|_2$ is the Euclidean norm.

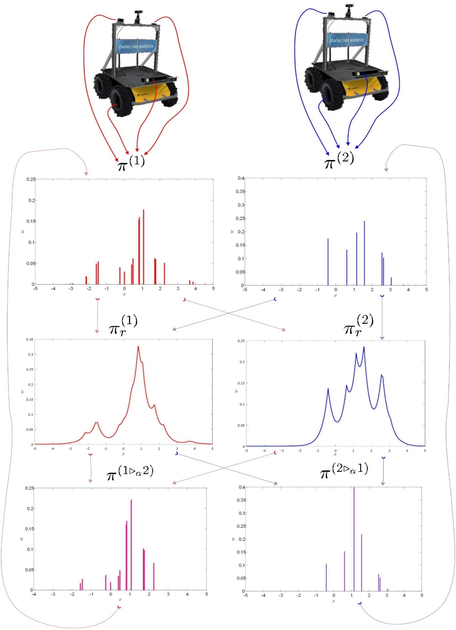

Figure 3: Illustration of the particles intersection algorithm. The two robots in the top use their sensor to produce the empirical approximations $\pi^{(1)}$ and $\pi^{(2)}$ of the filtering pdf. The empirical approximations are then regularized to $\pi_r^{(1)}$ and $\pi_r^{(2)}$. Each particles weights is updated by algorithm 1..

Algorithm 1 Interaction via particles intersection

Input: $\{x_k^{(i),1},\ w_k^{(i),1}\}_{i=1}^N$ and $\{x_k^{(i),2},\ w_k^{(i),2}\}_{i=1}^N$

Output: $\{x_k^{(i),1},\ v_k^{(i),1}\}_{i=1}^N$ and $\{x_k^{(i),2},\ v_k^{(i),2}\}_{i=1}^N$

for $j = 1 : N$ **do**

$\bar{v}_k^{(j),1} = \pi_r(x_k^{(j),1} \mid z_{0:k}^1) \triangleright_\alpha \pi_r(x_k^{(j),1} \mid z_{0:k}^2)$

$\bar{v}_k^{(j),2} = \pi_r(x_k^{(j),2} \mid z_{0:k}^1) \triangleright_\alpha \pi_r(x_k^{(j),2} \mid z_{0:k}^2)$

end for

for $j = 1 : N$ **do**

$v_k^{(j),1} = \bar{v}_k^{(j),1} / \left(\sum_{l=1}^N \bar{v}_k^{(l),1}\right)$

$v_k^{(j),2} = \bar{v}_k^{(j),2} / \left(\sum_{l=1}^N \bar{v}_k^{(l),2}\right)$

end for

Multiple Targets Tracking

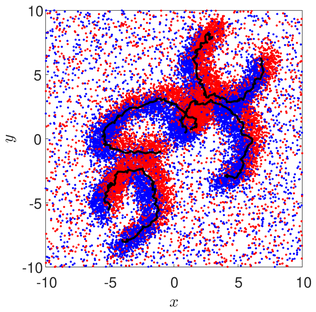

Figure 4: Trails of four moving objects and the accumulated clutter over that period of time. The black lines represent the actual path of the objects, and the red and blue dots represent the observations of the two sensors.

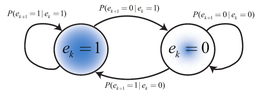

Figure 5: Here, $e_k^i \in \{0,1\}$ is a realization of a Bernoulli random variable indicating whether or not the ith object is present at time k. This Markov chain demonstrates the state shift of e_k^i.

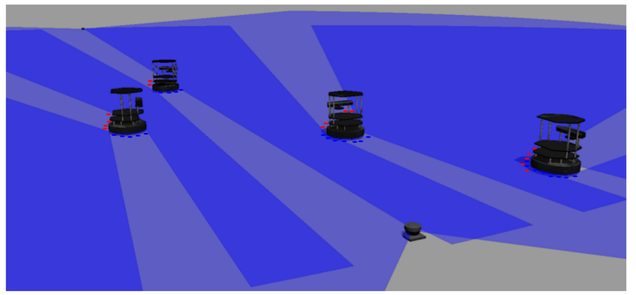

Figure 6: The Gazebo simulation environment with 4 manoeuvring robots as targets and on the bottom right and top left there are two laser scanners sensors tracking the targets. The blue and red dots demonstrates the observations of the two sensors, where the first PF uses the blue measurements and the second one uses use the red measurements.

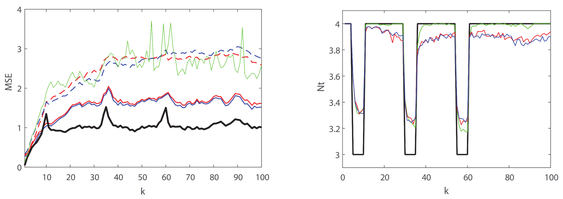

Figure 7: MSE errors evaluated using 100 Monte Carlo runs (left). The performance of a centralized PF that uses observations from both laser scanners is shown in black. The estimation errors of the interacting PFs are shown as the solid red and blue lines. The respective estimation errors of the non-interacting PFs are shown by the dashed red and blue lines. The MSE errors of the CI technique is shown in green. Estimated (colored lines) and actual (black line) number of objects (right). The red and blue lines are the estimated number of objects averaged over 100 Monte Carlo runs of the non-interacting PFs. The respective estimate of one of the interacting PFs is shown in green.

Cooperative Robots Localization

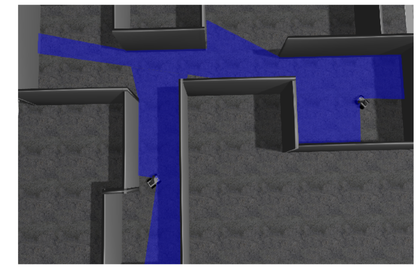

Figure 8: gazebo simulation of two robots navigating with a shared map.

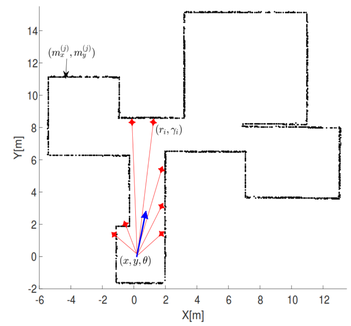

Figure 9: Demonstration of the given map for the simulation. The black dots are the map $\{m_j\}_{j=1}^{N_m}$, the red beams illustrates the laser scanners hits and the blue arrow shows the location of a robot.

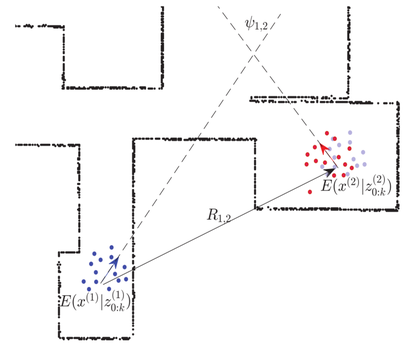

Figure 10: Illustration of the transformation step. The blue dots shows the first PF, the red dots shows the second PF and the bright blue dots represent the first PF transformation to the second one.

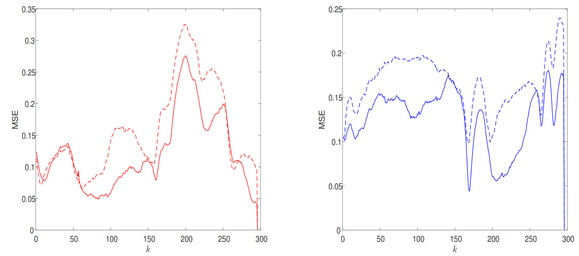

Figure 11: MSE errors evaluated using 100 Monte Carlo runs. The estimation errors of the interacting PFs are shown as the red and blue lines. The respective estimation errors of the non-interacting PFs are shown by the dashed red and blue lines.